

SUPPLEMENTAL FIGURE LEGENDS

Figure S1. Characterization of CCDC28B-deficient T cells. A,C,D. Immunoblot analysis of CCDC28B in lysates of control and CCDC28B KD or KO Jurkat cells (A) or of control and CCDC28B KD primary T cells (C), or of CCDC28B KD Jurkat cells transfected with a CCDC28B-GPF expression construct (D). The samples of control and CCDC28B KO Jurkat cells in the figure A belong to the same immunoblot. Actin was used as loading control. The migration of molecular mass markers is shown for each filter. Quantifications of the relative intensities of the CCDC28B-immunoreactive band (KD/KO vs ctr) are shown in the box ($n \geq 3$). **B.** Flow cytometric analysis (MFI) of surface CD3 on the same samples as in A and C ($n=3$). Error bars, SD. ***, $p < 0.001$; **, $p < 0.01$; *, $p < 0.05$ (Student's t-test).

Figure S2. CCDC28B is required for phosphotyrosine signaling in T cells activated by SEE-pulsed APC. A. Time course analysis of protein tyrosine phosphorylation in conjugates of control or CCDC28B KD Jurkat cells and SEE-pulsed Raji cells (APC). Conjugates were labelled with anti-CD3 and anti-PTyr antibodies, and the analysis was carried out on CD3⁺ cells ($n=2$). Error bars, SD. *, $p < 0.05$ (Student's t-test). **B.** Immunofluorescence analysis of CD3 ζ and pericentrin (centrosome marker) in 15-min conjugates of control or CCDC28B KD Jurkat cells and SEE-pulsed Raji cells (APC). The image shows an example of the observed dissociation of CD3⁺ endosomes from the centrosome during IS polarization in CCDC28B KD cells.

Figure S3. CCDC28B is required for immune synapse assembly. A,B,D. Immunofluorescence analysis of CD3 ζ (A) and tyrosine phosphoproteins (PTyr) (B) or F-actin (D) in 15 min-conjugates of control or CCDC28B KO Jurkat cells and SEE-pulsed Raji cells. The histograms show the quantification (%) of conjugates with CD3 ζ or PTyr staining at the T-cell:APC contact site (left), or the relative fluorescence of CD3 ζ , PTyr or F-actin at the T-cell:APC contact site compared to the remaining T-cell area (recruitment index) (right). **C.** Immunofluorescence analysis of the same samples as in A labelled for γ -tubulin. The histogram shows the quantification (%) of conjugates with γ -tubulin at the T cell:APC contact site. **E,F.** Immunofluorescence analysis in 15 min-conjugates of control or CCDC28B KO Jurkat cells and SEE-pulsed Raji cells co-stained for F-actin and WASH. The histograms show the quantification (%) of WASH⁺ dots positive for F-actin (E); and the co-localization (Mander's coefficient) of WASH with F-actin on individual dots (F). Measurements were taken on 60 conjugates from at least 3 independent experiments. Error bars, SD. ***, p<0.001; **, p<0.01; *, p<0.05 (Student's t-test).

Figure S4. The endosomal pool of CD3 is expanded in activated primary T cells. A. Scheme of the experimental protocol used to generate primary T cell blasts from SEA/SEB/SEE-pulsed PBMC. **B.** Immunofluorescence analysis of CD3 ζ in primary T cells, either immediately after purification or after activation (see panel A). Cells were fixed and stained either without or with a permeabilization step to visualize plasma membrane-associated CD3 ζ or total CD3 ζ , respectively. Representative images are shown. Size bar, 5 μ m.

Figure S5. CCDC28B is required for recruitment of the actin regulator WASH and its adaptor FAM21 to recycling TCRs. **A.** Immunofluorescence analysis of WASH in 15 min-conjugates of control or CCDC28B KD primary T cells and SEA/SEB/SEE-pulsed Raji cells (APC) co-stained for F-actin. The histograms show the mean distance of WASH⁺ dots from the T-cell:APC contact site (top) and the co-localization of WASH with F-actin on individual dots (bottom, Mander's coefficient) (n=3). **B,C.** Immunofluorescence analysis of recycling TCRs (tCD3) in control or CCDC28B KD primary T cells conjugated for 15 min with SEA/SEB/SEE-pulsed Raji cells (APC) and co-stained for WASH (B) or FAM21 (C). Before conjugation, cells were added with anti-CD3 ϵ mAb (OKT3) and incubated at 37°C for 2 h to allow for internalization of CD3-Ab complexes. Following acid-stripping to remove residual anti-CD3 mAb bound at the cell surface. Conjugates were permeabilized/fixed and stained with primary antibodies for WASH (B) or FAM21 (C) and secondary fluorescently-labelled antibodies. For each panel the histograms show the quantification of tCD3⁺ dots positive for WASH or FAM21 (top, %); and the co-localization of tCD3 with WASH or FAM21 on individual dots (bottom, Mander's coefficient). Measurements were taken on 60 conjugates from at least 3 independent experiments. Size bar, 5 μ m. Error bars, SD. ***, p<0.001; **, p<0.01 (Student's t-test).

Figure S6. Constructs and protocols used to study CCDC28B interactors. **A.** Experimental protocol for the purification of tagged recycling CD3 (tCD3). **B.** Domain organization of FAM21C, WASH and CCDC28, and schematic representation of the GST fusion proteins used in this study. **C.** Protein-protein interactions known to occur among the retromer core component VPS35 (the other two components

VPS26 and VPS29 are shown in grey), FAM21C and WASH at early endosomes (EE). **D.** Interactions of CCDC28B with retromer and FAM21.

Figure S7. CCDC28 associates with VPS35 and WASH and is required to couple WASH to ARPC3 and α -tubulin. **A,B.** Immunoblot analysis of VPS35-specific (A) or WASH-specific (B) immunoprecipitates from post-nuclear supernatants of Jurkat cells. Immunoprecipitates carried out with non-immune Abs were used as negative control (neg ctr) (n=3). **C.** Immunoblot analysis of WASH-specific immunoprecipitates from post-nuclear supernatants of control or CCDC28B KD Jurkat cells. Immunoprecipitates carried out with non-immune Abs were used as negative control (neg ctr). The quantifications of the relative intensities of the immunoreactive bands (KD vs ctr) are shown in the box (n=3). **D.** Immunoblot analysis of GSH-Sepharose pull-down assays on post-nuclear supernatants of Jurkat cells using either GST fusion proteins encoding the N-terminal (GST-FAMn) and C-terminal (GST-FAMc) portions of the L-F-[D/E](3-10)-L-F repeat-rich tail of FAM21 (see schemes in figure S6B). Recombinant GST was used as negative control. The Ponceau staining of the filter is shown (n=3). Total post-nuclear supernatants (lys) were included in all gels. The migration of molecular mass markers is shown for each filter. Error bars, SD. ***, p<0.001; *, p<0.05 (Student's t-test).

Figure S8. Characterization of T cells from the COVID patient-derived samples used for the experiments in figure 7. **A,B.** Flow cytometric analysis (MFI) of surface CD3 (A) and immunoblot analysis of CCDC28B (B) on the same samples as in figure 7A. The histograms shows the quantification of the intensities of the

CCDC28B-immunoreactive bands, normalized to actin used as loading control. All gels included a lysate of the same healthy donor sample to allow for comparison. **C.** Immunofluorescence analysis of CD3 ζ , tyrosine phosphoproteins or F-actin in 15-min conjugates of HD (4, the same as in figure 7) and patient #5 T cells (non-CVID, homozygous for the wild-type *ccdc28b* allele) and Raji cells pulsed with a mix of SEA, SEB and SEE. The scattered dot plot shows the quantification (%) of conjugates with CD3 ζ , PTyr or F-actin staining at the immune synapse (n conjugates =100).

Figure S9. Scheme of CCDC28B-dependent interactions at early endosomes that promote TCR recycling. CCDC28B couples FAM21 to VPS35 (retromer) at early endosomes through an interaction involving binding of the CC domain of CCDC28B to VPS35 and the molecular determinant that contains R25 to the C-terminal domain of FAM21. This allows for WASH recruitment and local actin polymerization to provide force for abscission of TCR-enriched endosomes. These are coupled to microtubules through WASH and FAM21 for retrograde transport to the centrosome that has translocated to the T cell:APC contact site during immune synapse formation. The ability of CCDC28B to couple FAM21/WASH to retromer is lost in the CCDC28B^{R25W} T-CVID-associated variant, leading to impaired retrograde trafficking and defective immune synapse assembly.

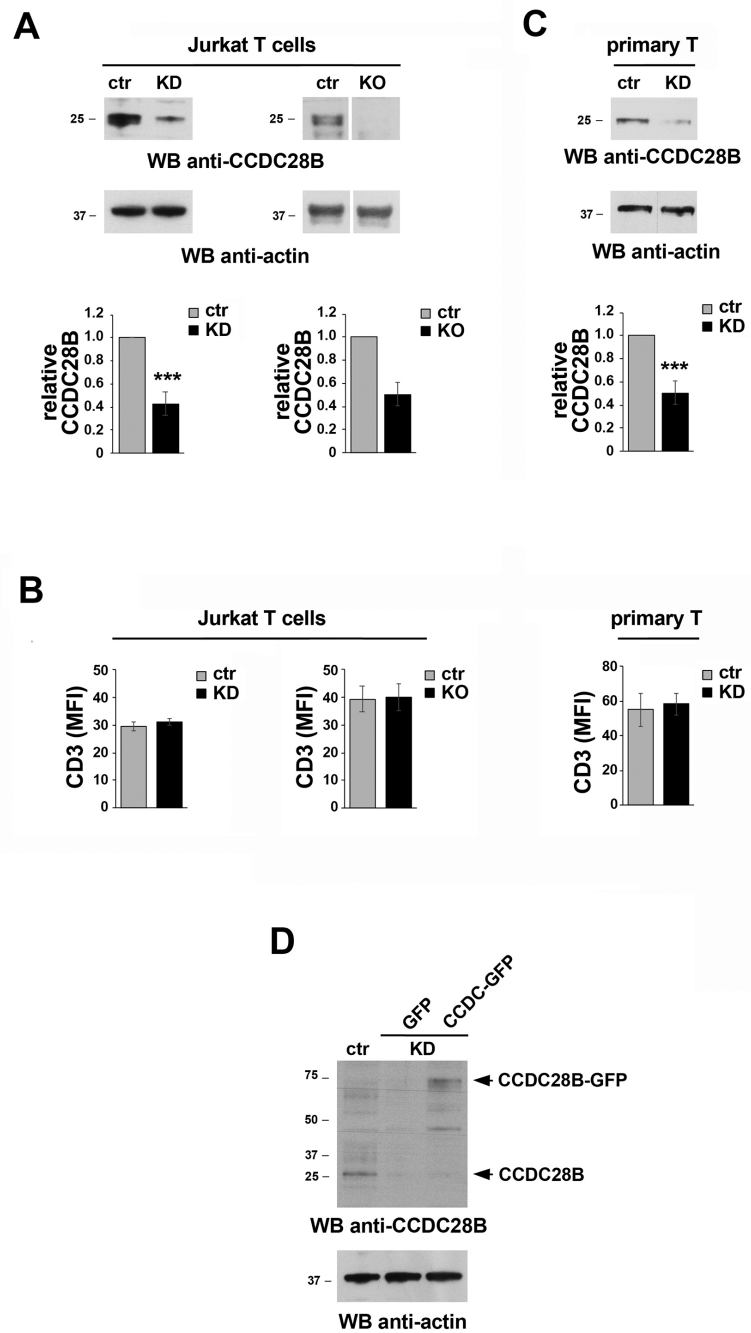


FIGURE S1

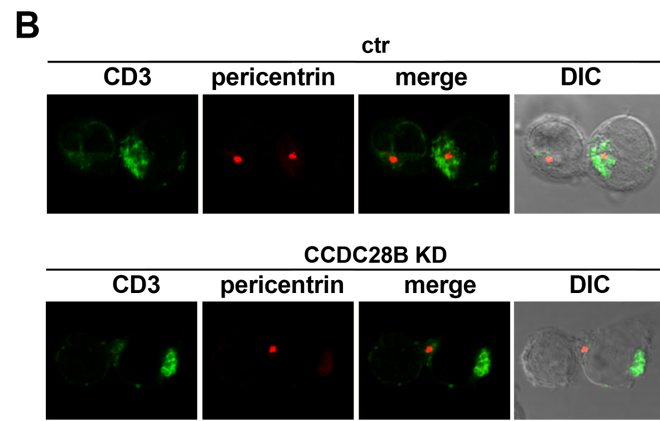
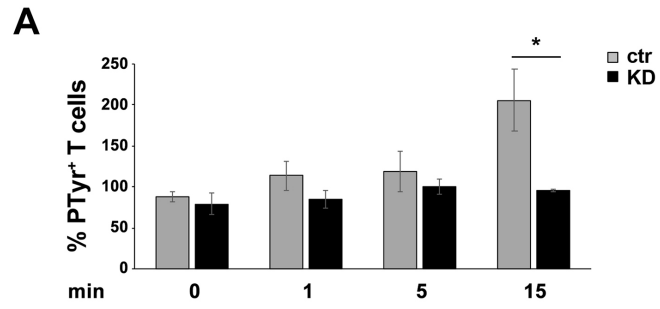


FIGURE S2

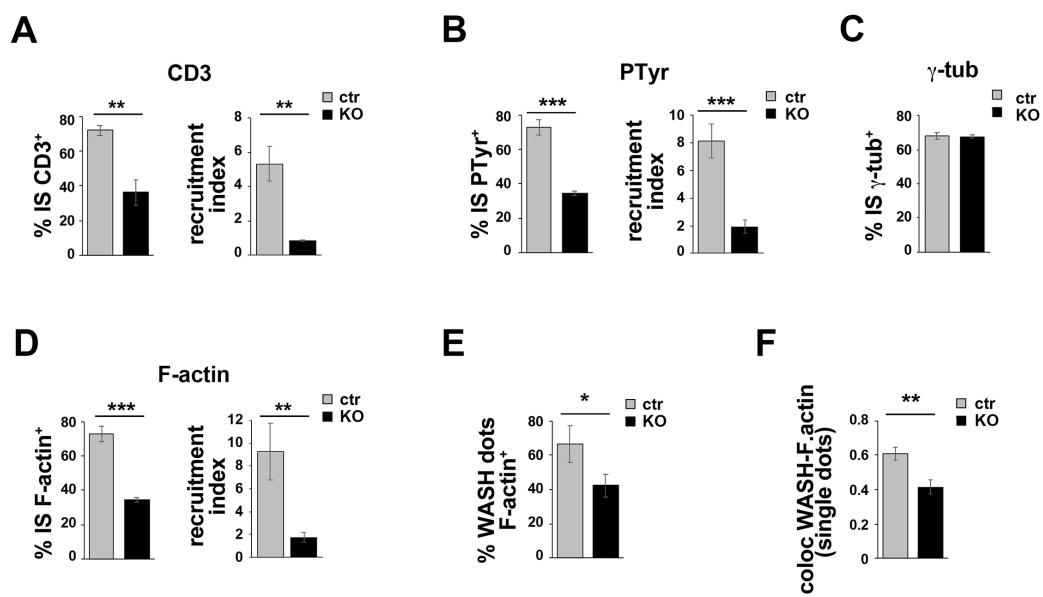


FIGURE S3

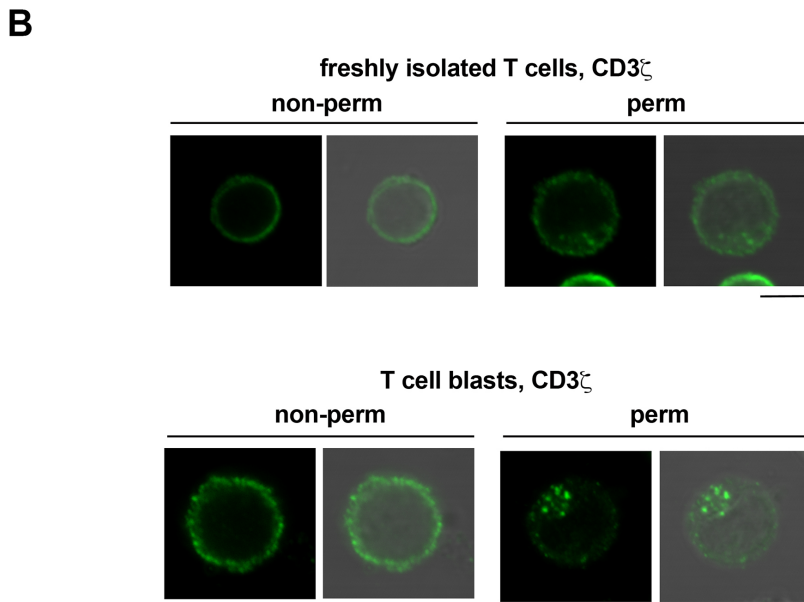
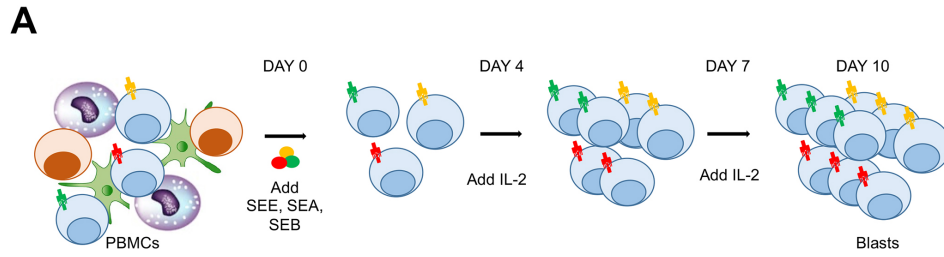


FIGURE S4

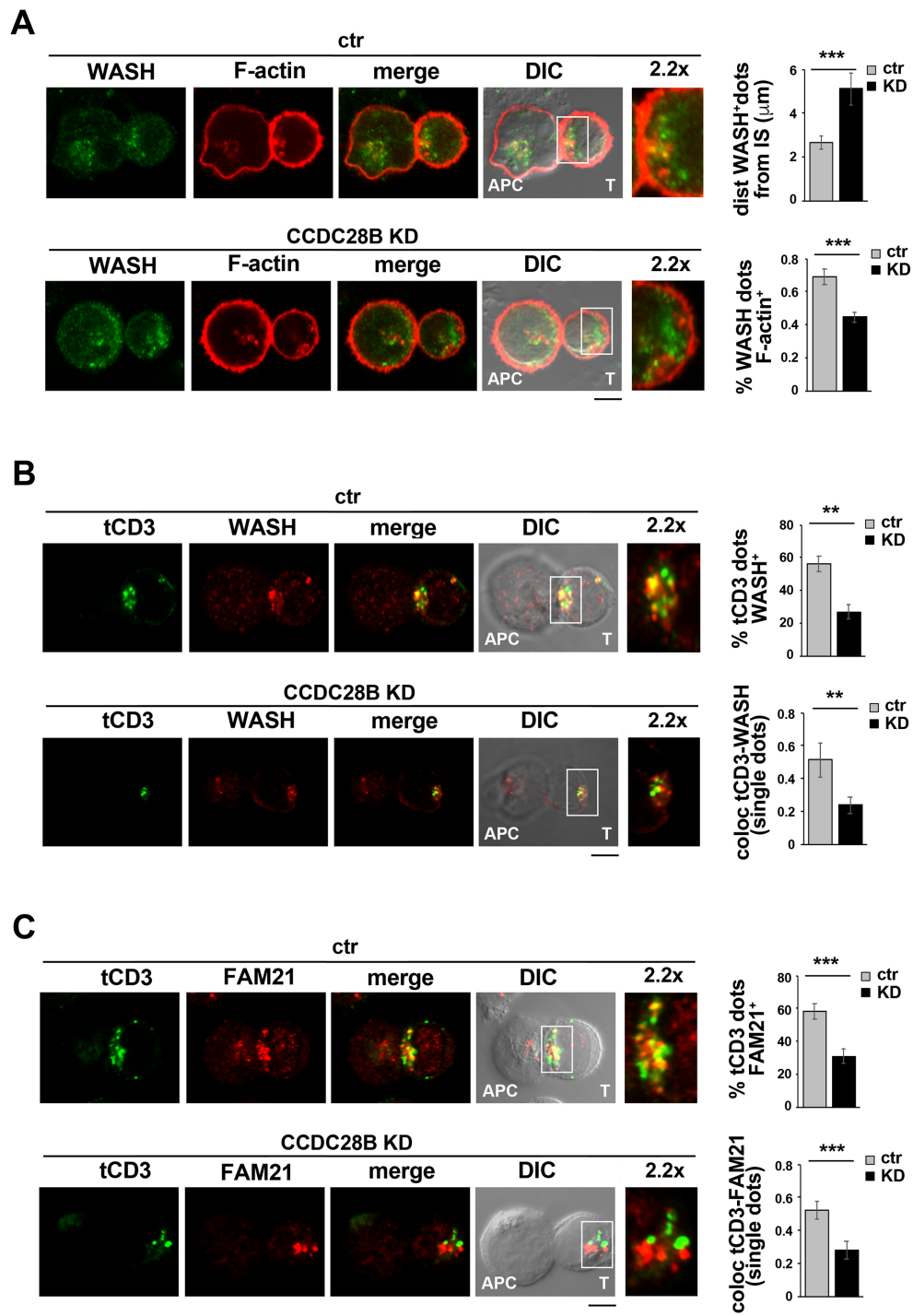


FIGURE S5

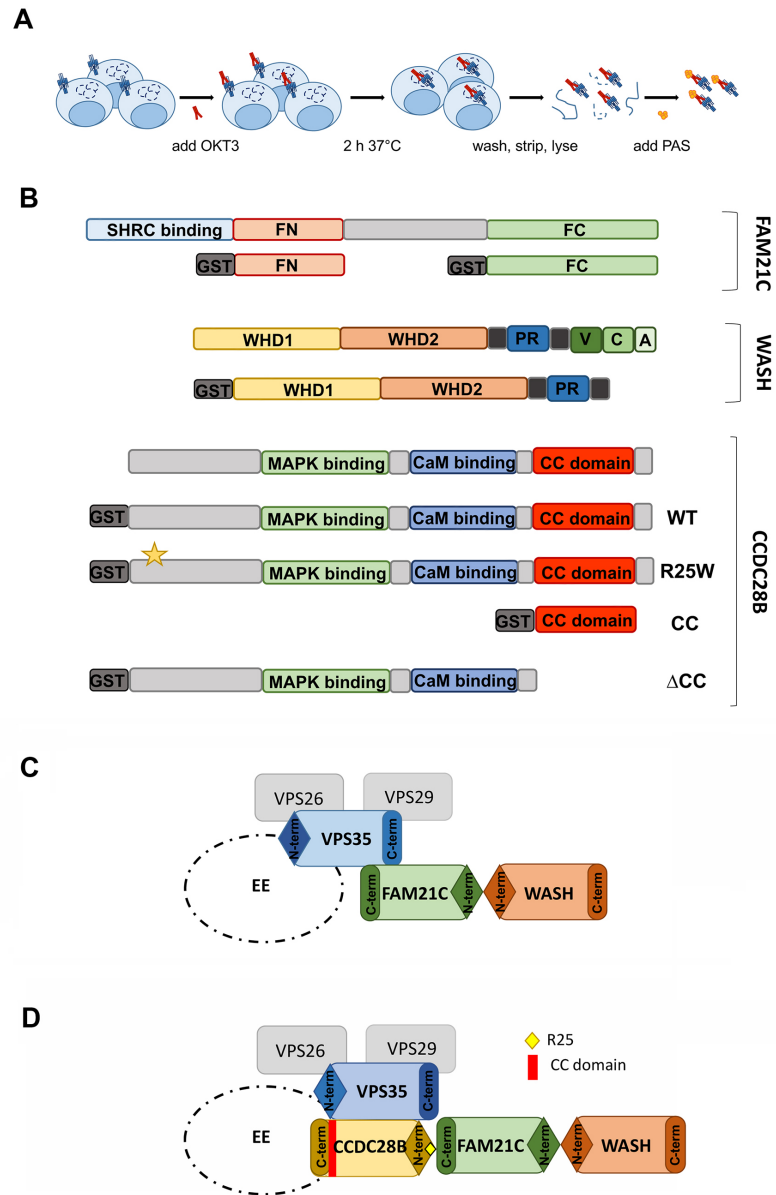


FIGURE S6

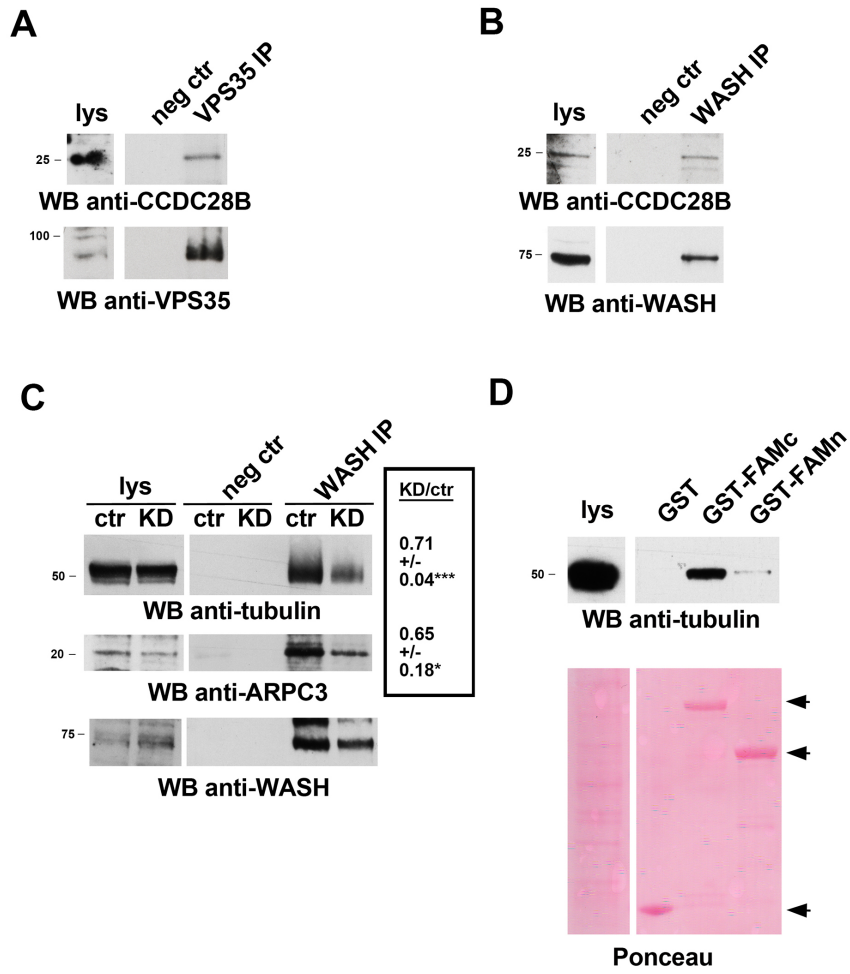


FIGURE S7

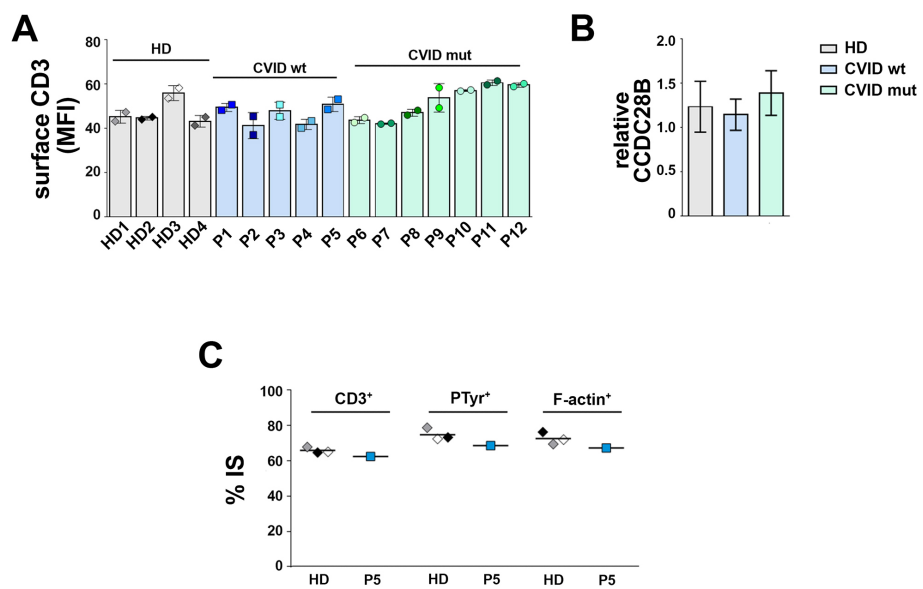


FIGURE S8

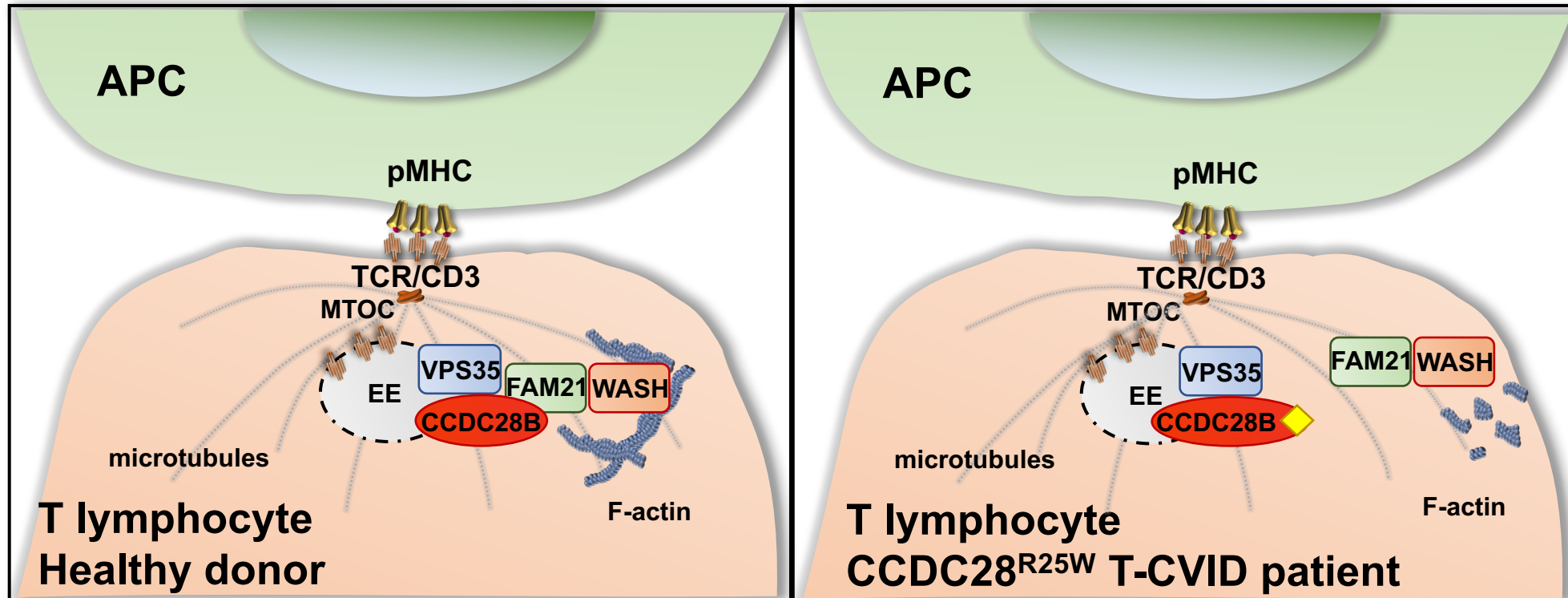


FIGURE S9

Table S1. Commercial antibodies

Antibody	Host Species	Catalogue number	Source	WB dilution	IF dilution	IP dilution
Anti-CCDC28B	rabbit	NBP2-15747	Novus Biologicals	1:500	1:100	-
Anti-γtub	mouse	T6557	Sigma Aldrich	-	1:100	-
Anti-Rab5	rabbit	PA3-915	Thermo Fisher Scientific	-	1:200	-
Anti-Rab5	mouse	610725	BD	-	1:50	-
Anti-Rab11a	rabbit	2413	Cell Signaling	-	1:50	-
Anti-GM130	mouse	610822	BD	-	1:100	-
Anti-CD3ζ	mouse	Sc-1239	Santa Cruz	1:50	1:50	-
Anti-P-Tyr	mouse	05-321	Merk Millipore	-	1:100	-
Alexa Fluor 488 phalloidin		A12379	Invitrogen	-	1:40	-
phalloidin TRITC		P-1951	Sigma Aldrich	-	1:500	-
Anti-Wash	rabbit	PA5-51731	Invitrogen	1:500	1:100	-
Anti-Wash	mouse	SAB4200552	Sigma Aldrich	-	1:100	1:500
Anti-GFP	rabbit	A11122	Invitrogen	1:500	1:200	-
Anti-GFP	mouse	A11120	Invitrogen	-	1:200	1:500
Anti-Fam21	rabbit	GTX120832	GeneTex	-	1:400	-
Anti-Fam21C	mouse	H00253725-B01P	Novus Biologicals	1:500	-	-
Anti-VPS35	mouse	sc-374372	Santa Cruz	1:500	1:100	1:200
Anti-β-tubulin	mouse	T5293	Sigma Aldrich	1:500	1:200	-
Anti-p21-ARC	rabbit	sc-68396	Santa Cruz	1:500	-	-
Anti-IgG isotype ctr	mouse	31903	Invitrogen	-	-	1:1000
Anti-actin	mouse	MAB1501	Merk Millipore	1:10000	-	-
Anti-pericentrin	rabbit	Ab4448	Abcam	-	1:200	-

Western Blot (WB), Immunofluorescence (IF), Immunoprecipitation (IP)

Table S2. List of the primers used in this study

Sanger sequencing	Forward 5'-3'	Reverse 5'-3'
CCDC28B	TTT GTG GGG GTT GCT TCC CT	ACC CAC CTC TTG AAC TTG GC
MKKS (BBS6)	AAC CTG CCT GTA TGC TCA CC	AAG CAG CTG GTC CAA GAC T
BBS10	TCA GGA CAC AGT TGC AGA GA	CCC CTT GTT GAA TAA GCA GTG G
SDCCAG8 (BBS16)	GTG TGG AGT TTA AGA TAA TGT TAA GGT	ATT CCG CAG CAA TTC CCC TT
WDR35 (IFT121)	TCT CTG TGA AGT GAT TGG TGG T	GCT AGC TCC TAA AAC AAG ACA GC
Cloning primers	Forward 5'-3'	Reverse 5'-3'
CCDC28B wt (pEGFP-N1)	CCG CTC GAG CGA TGG ATG ACA AAA A	CGC GGA TCC CTA CGC AGC GGA CTG C
CCDC28B mut (pEGFP-N1)	CCA GGC ACA CTA TGG AGG GTC CCTG	CAG GGA CCC TCC ATA GTG TGC CTGG
CCDC28B wt/mut (pGEX-6P-2)	CCG GAA TTC CAT GGA TGA CAA AAA GAA GAA AC	CCT CGA GGC TAC GCA GCG GAC TG
CCDC28B ΔCC (pGEX-6P-2)	CCG GAA TTC CAT GGA TGA CAA AAA GAA GAA AC	CCT CGA GGC TAT GGC AGC CCC TC
CCDC28B CC (pGEX-6P-2)	CCG GAA TTC CGA GGA GCA GAA GAA G	CCG CTC GAG GCT AGA TAG AAT TAC TGA G

CRISPR Cas9
gRNA *ccdc28b*

GAACTTGGCCCGCTGCTTGG

RNA interference

esiRNA targeting RLUC (EHURLUC)

CCDC28B-specific esiRNAs (EHU082341)
